

Research Article

Synthesis, Structural, Electrical, and Thermal Studies of $\text{Pb}_{1-x}\text{Ba}_x\text{Nb}_2\text{O}_6$ ($x = 0.0$ and 0.4) Ferroelectric Ceramics

Shiv K. Barbar¹ and M. Roy²

¹ Center for Condensed Matter Sciences, National Taiwan University, Taipei-10617, Taiwan

² Department of Physics, M.L. Sukhadia University, Udaipur-313002, Rajasthan, India

Correspondence should be addressed to Shiv K. Barbar, barbar_shivkumar@yahoo.co.in

Received 26 June 2012; Accepted 23 July 2012

Academic Editors: S. Bernik, V. Fruth, and S. Marinell

Copyright © 2012 S. K. Barbar and M. Roy. This is an open access article distributed under the Creative Commons Attribution License, which permits unrestricted use, distribution, and reproduction in any medium, provided the original work is properly cited.

The polycrystalline ceramic samples of lead barium niobate with general formula $\text{Pb}_{1-x}\text{Ba}_x\text{Nb}_2\text{O}_6$ ($x = 0.0$ and 0.4) were prepared by conventional solid state reaction method. The room temperature X-ray diffraction patterns reveal that both of the samples have orthorhombic crystal structure with space group Cm2m. The dielectric constant and dissipation factor were measured as a function of frequency (100 Hz-2 MHz) and temperature (RT-660K). The DC electrical conductivity of both the samples was measured from RT to 660 K. The activation energies calculated from $\log \sigma$ versus $1000/T$ curves in ferroelectric phase of the compounds are 1.09 eV for pure ($x = 0.0$) sample and 1.36 eV for Ba-substituted ($x = 0.4$) sample. The values of activation energies show that the substitution of Ba^{2+} ion on Pb^{2+} ion site increases the resistivity of pure PbNb_2O_6 ($x = 0.0$) ceramic. The modulated differential scanning calorimetry (MDSC) has been used to investigate the phase transition temperature of both the compounds and also to see the effect of Ba^{2+} ion substitution on the phase transition temperature, specific heat, and other thermal parameters of the compound.

1. Introduction

Lead niobate (PbNb_2O_6) is one of the first crystals of the tungsten bronze-type structure which was first reported as ferroelectric [1]. It is well known that the tungsten bronze niobates generally indicate a relaxor ferroelectric nature. These materials crystallize in a variety of structures including tetragonal tungsten bronze (TTB), hexagonal tungsten bronze (HTB), and intergrowth tungsten bronze (ITB) [2].

The synthesis and phase identification of the piezoelectric/ferroelectric phase of lead niobate is difficult, that a few competing phases and compounds tend to form during the preparation [3–10]. Crystallographic studies revealed that at room temperature material is found in ferroelectric orthorhombic phase and above the Curie temperature (843 K) it shows paraelectric tetragonal phase [11–14]. The activation energies calculated from dc conductivity measurement from different formalism showed the ionic-type conduction in doped niobate $\text{Pb}_{0.74}\text{K}_{0.13}\text{Y}_{0.13}\text{Nb}_2\text{O}_6$ compound [15]. Thermal characterization through DSC

technique for pure PbNb_2O_6 showed the Curie temperature at 843 K in heating profile and at 826 K in cooling process [16].

Due to high Curie temperature and low-quality factor, the material is useful for fabrication of ultrasonic transducers for high-temperature applications where the PZT and other piezoelectric materials cannot be used [5, 17]. The present paper report on the synthesis, structural, electrical, and thermal properties of pure and 40% Ba-substituted lead niobate compounds.

2. Experimental

The polycrystalline ceramic samples of $\text{Pb}_{1-x}\text{Ba}_x\text{Nb}_2\text{O}_6$ ($x = 0.0$ and 0.4) were prepared by high-temperature solid state reaction technique. The constituent oxides, PbO (High Media, 99.9%), BaO (CDH Mumbai, 99.9%) and Nb_2O_5 (High Media, 99.9%) were mixed together according to stoichiometric amounts in a mortar and pestle under liquid

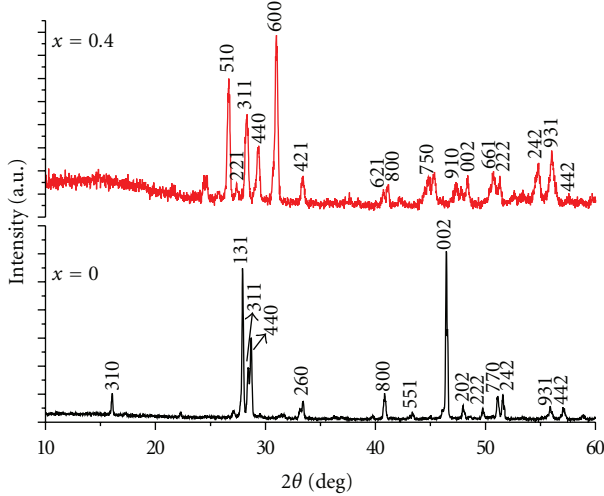


FIGURE 1: X-ray diffraction pattern of $\text{Pb}_{1-x}\text{Ba}_x\text{Nb}_2\text{O}_6$ ($x = 0.0$ and 0.4).

medium to make a homogeneous mixture. The mixtures were calcined at 1073–1273 K for 4 hours in a silica crucible in air atmosphere. The process of firing and mixing was repeated for a number of times. The product was then pressed into pellet form by applying pressure of 498 MPa in a hydraulic press. Finally, these pellets were sintered at 1553–1573 K for 1 hour and cooled to RT very fastly. The room temperature (RT) X-ray diffraction patterns of the sintered pellets were collected using a Rigaku X-ray diffractometer with $\text{CuK}\alpha$ radiation and nickel filter in a wide range of 2θ from 10° to 60° with a scanning rate of 2° per minute and step size of 0.02° . The instrument was calibrated using the pure silicon sample provided with the instrument. Before measuring the electrical properties both the samples were electroded with silver paint. The dielectric constant and dissipation factor as a function of frequency and temperature were measured in air atmosphere using Hioki LCR 3532-50 Hi Tester. The dc electrical conductivity measurement was carried out on laboratory made set up using two probe method. The modulated DSC measurement was carried out on TA instruments model 2910 MDSC equipment from RT to 853 K in inert (N_2) atmosphere with a heating rate of 5 K/min and ± 0.75 K modulation per 60 second.

3. Results and Discussion

Figure 1 shows the X-ray diffraction patterns of $\text{Pb}_{1-x}\text{Ba}_x\text{Nb}_2\text{O}_6$ ($x = 0.0$ and 0.4) compounds. All the diffraction peaks, indexed with space group $\text{Cm}2\text{m}$ in orthorhombic crystal structure using Rietveld refinement program Fullprof, are well matching with JCPDS card no. 11–0122 of the PbNb_2O_6 compound. The pseudo-Voigt function was chosen for the profile shape refinement. The refined cell parameters are found to be $a = 17.682 \text{ \AA}$, $b = 17.953 \text{ \AA}$, and $c = 3.841 \text{ \AA}$ for pure compound ($x = 0.0$) and $a = 17.254 \text{ \AA}$, $b = 17.505 \text{ \AA}$, and $c = 3.736 \text{ \AA}$ for Ba-substituted compound ($x = 0.4$). From the figure, it is clear that the X-ray diagram of the substituted compound is quite similar to that of the pure compound except few reflection

TABLE 1: Comparison between d -observed and d -calculated values for $\text{Pb}_{1-x}\text{Ba}_x\text{Nb}_2\text{O}_6$ ($x = 0.0$ and 0.4).

hkl	$x = 0.0$		$x = 0.4$	
	$t = 40 \text{ nm}$	$t = 40 \text{ nm}$	$t = 30 \text{ nm}$	$t = 30 \text{ nm}$
	$d\text{-obs (\AA)}$	$d\text{-cal (\AA)}$	$d\text{-obs (\AA)}$	$d\text{-cal (\AA)}$
310	5.6023	5.5999	—	—
221	—	—	3.1939	3.1925
131	3.1810	3.1797	—	—
311	3.1622	3.1596	3.0856	3.0843
440	3.1508	3.1495	3.0733	3.0721
600	—	—	2.8768	2.8756
260	2.8355	2.8343	—	—
421	—	—	2.6889	2.6877
621	—	—	2.2062	2.2054
800	2.2111	2.2103	2.1575	2.1567
551	2.1075	2.1067	—	—
750	—	—	2.0162	2.0154
910	—	—	1.9064	1.9057
002	1.9211	1.9204	1.8690	1.8683
202	1.8773	1.8766	—	—
661	—	—	1.7966	1.7960
222	1.8376	1.8369	1.7882	1.7875
770	1.8004	1.7997	—	—
242	1.7320	1.7314	1.6858	1.6852
931	1.6795	1.6789	1.6378	1.6372
442	1.6402	1.6396	1.5969	1.5963

peaks which are not similar in both the cases. It has also been observed that there is little shift in the peak positions of the substituted compound which is responsible for the corresponding minor change in the structural parameters.

There is a good agreement between the observed and calculated interplanar spacings (d -values) for both the compounds and are shown in Table 1. From the table, it is found that with the substitution of Ba^{2+} ion the change in d -values are not much different insignificant.

The average crystallite sizes as determined from the XRD using the Scherrer formula $t = 0.89\lambda/\beta\cos\theta$, where β = full width at half maxima and λ = wavelength of radiation used, are shown in Table 1.

The frequency variation of the dielectric constant (ϵ') and dissipation factor (ϵ'') of both samples are plotted in Figures 2(a) and 2(b). It was found that with the increase of frequency both the dielectric constant and dissipation factor decrease very fast up to frequency of 10 kHz which is due to the space charge contribution. After 10 kHz, ϵ' and ϵ'' decrease slowly due to the ionic and electronic charge contribution up to the measured frequency range of 2 MHz. These variations of ϵ' and ϵ'' with frequency indicate the characteristics of relaxor behavior of the material. Figures 3(a) and 3(b) show the temperature dependence of the ϵ' and ϵ'' for both the compounds at a frequency of 100 kHz. From the Figure 3(a), it is observed that the values of ϵ' of both the compounds are almost temperature independent or constant up to the temperature of 450 K and then increases. The pure

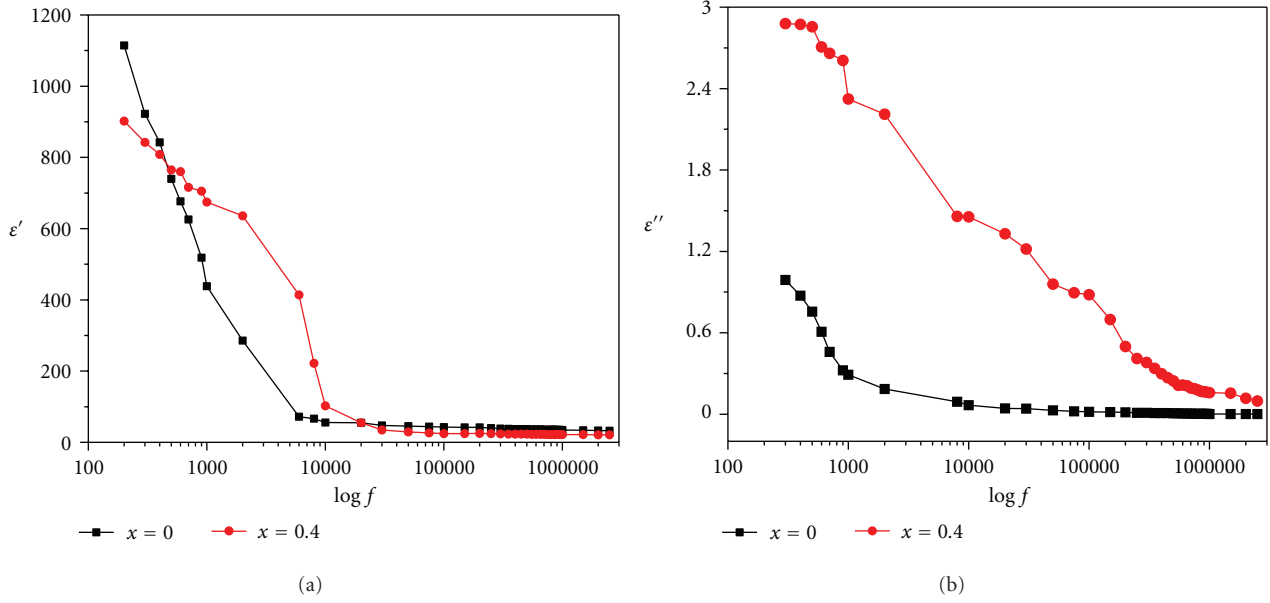


FIGURE 2: (a) Dielectric constant versus $\log f$ curves of $\text{Pb}_{1-x}\text{Ba}_x\text{Nb}_2\text{O}_6$ ($x = 0.0$ and 0.4). (b) Dissipation factor versus $\log f$ curves of $\text{Pb}_{1-x}\text{Ba}_x\text{Nb}_2\text{O}_6$ ($x = 0.0$ and 0.4).

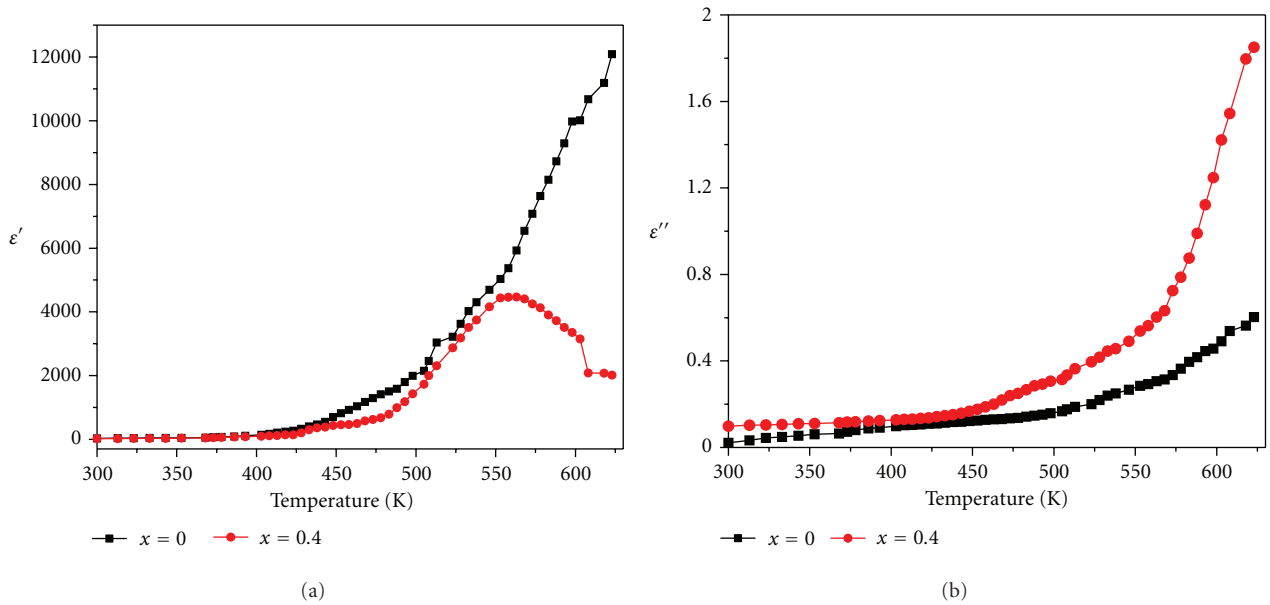


FIGURE 3: (a) Dielectric constant versus temperature curves of $\text{Pb}_{1-x}\text{Ba}_x\text{Nb}_2\text{O}_6$ ($x = 0.0$ and 0.4). (b) Dissipation factor versus temperature curves of $\text{Pb}_{1-x}\text{Ba}_x\text{Nb}_2\text{O}_6$ ($x = 0.0$ and 0.4).

compound ($x = 0.0$) does not show any transition/dielectric anomaly up to the measured temperature range. With the substitution of Ba^{2+} ion in place of Pb^{2+} ion ($x = 0.4$), the overall dielectric constant decreases and shows a broad and diffuse peak at 560 K and then decreases again up to the measure temperature range of 660 K. This broad and diffuse dielectric response may be correlated with the fine grain size of the compound consistent with the literature report [18, 19] as well as observed in the case of PZT [20]. The temperature variation of the dissipation factor

(ϵ'') for both the compounds at a frequency of 100 kHz is shown in Figure 3(b). The dissipation factor shows almost same trend as dielectric constant with no indication of any peak/anomaly up to the measured temperature range.

Figure 4 shows the temperature dependence of dc conductivity (σ_{dc}) for both of the compounds where \log of conductivity was plotted against inverse of temperature. Since, the conductivity is too small to be measured below the temperature of 463 K for both the compounds and hence the results are plotted for elevated temperature range

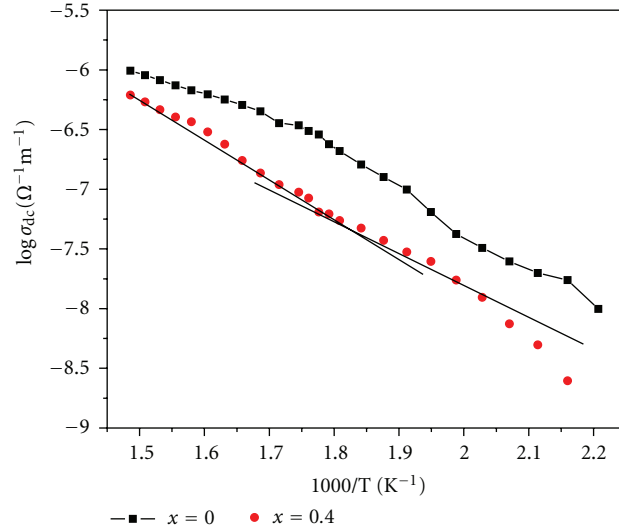


FIGURE 4: DC conductivity versus $1000/T$ curves of $\text{Pb}_{1-x}\text{Ba}_x\text{Nb}_2\text{O}_6$ ($x = 0.0$ and 0.4).

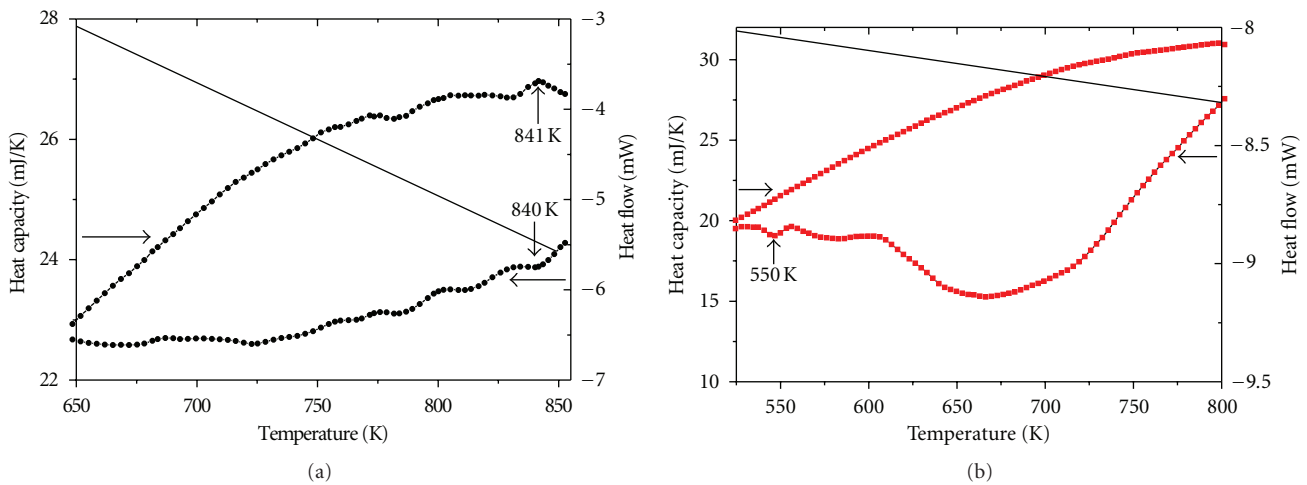


FIGURE 5: (a) Heat capacity and heat flow versus temperature curves of $\text{Pb}_{1-x}\text{Ba}_x\text{Nb}_2\text{O}_6$ ($x = 0.0$). (b) Heat capacity and heat flow versus temperature curves of $\text{Pb}_{1-x}\text{Ba}_x\text{Nb}_2\text{O}_6$ ($x = 0.4$).

from 463 K to 660 K. Above 463 K, the conductivity of both samples increase up to the measured temperature range. By measuring the slope of the curves and using the relation $\sigma = \sigma_0 \exp[-E_a/kT]$, (where k is Boltzmann constant, σ_0 is preexponential factor and E_a is the activation energy) the activation energies of both the samples were determined. The average activation energy calculated for pure compound is 1.09 eV while the same for Ba-substituted compound are 1.36 eV in ferroelectric phase (below transition temperature, 560 K) and 1.22 eV in paraelectric phase (above transition temperature, 560 K). The low value of activation energy in high temperature region ($E_a = 1.22$ eV) may be due to the oxygen ion vacancies which might be the main carrier in the electrical conduction process.

The MDSC curves of the $\text{Pb}_{1-x}\text{Ba}_x\text{Nb}_2\text{O}_6$ ($x = 0.0$ and 0.4) compounds are shown in Figures 5(a) and 5(b). From the Figure 5(a), it is clear that the pure compound ($x = 0.0$) shows an exothermic peak at 841 K in heat capacity curve and an endothermic peak at 840 K in heat flow curve. These exo- and endothermic peaks around $568^\circ\text{C}/567^\circ\text{C}$ (841 K/840 K) are consistent with the reported ferro to paraelectric phase transition temperature ($T_c = 843$ K) [2]. When the Ba^{2+} ion (40%) is substituted in the Pb^{2+} ion site, the T_c peak shifted from 568°C (841 K) to 277°C (550 K) Figure 5(b). The shift in T_c value from 841 K to 550 K is consistent with our dielectric result. It is surprising that the heat capacity curve does not show any anomaly/transition around 550 K. This change in T_c for Ba-substituted compound may be due

to the difference in ionic radii of Pb^{2+} and Ba^{2+} as discussed in our earlier papers [21–23] as well as their different thermal characteristics. The calculated values of entropy change (ΔS) are $1.05 \text{ JK}^{-1} \text{ g}^{-1}$ and $0.88 \text{ JK}^{-1} \text{ g}^{-1}$ for $x = 0.0$ and $x = 0.4$ compounds, respectively, at phase transition temperature.

4. Conclusion

From the above studies, it is concluded that both samples exhibit single ferroelectric orthorhombic phase with space group $\text{Cm}2\text{m}$. Although the Ba-substitution is responsible for shifting in peak positions but both of the compounds shows same crystal structure. The high dielectric constant and high Curie temperature of pure lead niobate is suitable for high temperature piezoelectric transducers applications. With the substitution of isoelectronic cation (Barium) on Pb-ion site, the binding strength and thermal stability increases as well as the lattice parameters, crystallite size, dielectric constant, transition temperature, and dc conductivity decreases. The increase in binding strength and thermal stability as well as the decrease in transition temperature are useful parameters for eventual functionality of the materials for device application.

Acknowledgments

The authors are thankful to Dr. A. M. Awasthi and Suresh Bhardwaj of UGC-DAE-CSR Indore for providing MDSC measurement facility.

References

- [1] G. Goodman, "Ferroelectric properties of lead metaniobate," *Journal of the American Ceramic Society*, vol. 36, pp. 368–372, 1953.
- [2] V. Hornebecq, C. Elissalde, F. Weill, A. Villesuzanne, M. Menetrier, and J. Ravez, "Study of disorder in a tetragonal tungsten bronze ferroelectric relaxor: a structural approach," *Journal of Applied Crystallography*, vol. 33, no. 4, pp. 1037–1045, 2000.
- [3] M. Venet, A. Vendramini, F. L. Zabetto, F. Guerrero, D. Garcia, and J. A. Eiras, "Piezoelectric properties of undoped and titanium or barium-doped lead metaniobate ceramics," *Journal of the European Ceramic Society*, vol. 25, no. 12, pp. 2443–2446, 2005.
- [4] H. S. Lee and T. Kimura, "Effects of microstructure on the dielectric and piezoelectric properties of lead metaniobate," *Journal of the American Ceramic Society*, vol. 81, no. 12, pp. 3228–3236, 1998.
- [5] J. Soejima, K. Sato, and K. Nagata, "Preparation and characteristics of ultrasonic transducers for high temperature using PbNb_2O_6 ," *Japanese Journal of Applied Physics, Part 1*, vol. 39, no. 5, pp. 3083–3085, 2000.
- [6] H. S. Lee and T. Kimura, "Improvement of piezoelectric property due to microstructural control in lead metaniobate," *Journal of the Korean Physical Society*, vol. 32, no. 3, pp. S1198–S1200, 1998.
- [7] S. Ray, E. Günther, and H. J. Ritzhaupt-Kleissl, "Manufacturing and characterization of piezoceramic lead metaniobate PbNb_2O_6 ," *Journal of Materials Science*, vol. 35, no. 24, pp. 6221–6224, 2000.
- [8] Y. M. Li, L. Cheng, X. Y. Gu, Y. P. Zhang, and R. H. Liao, "Piezoelectric and dielectric properties of PbNb_2O_6 -based piezoelectric ceramics with high Curie temperature," *Journal of Materials Processing Technology*, vol. 197, no. 1–3, pp. 170–173, 2008.
- [9] F. Guerrero, Y. Leyet, M. Venet, J. de Los, and J. A. Eiras, "Dielectric behavior of the PbNb_2O_6 ferroelectric ceramic in the frequency range of 20 Hz to 2 GHz," *Journal of the European Ceramic Society*, vol. 27, no. 13–15, pp. 4041–4044, 2007.
- [10] W. N. Lawless, "Specific heats of lead and cadmium niobates at low temperatures," *Physical Review B*, vol. 19, no. 7, pp. 3755–3760, 1979.
- [11] M. H. Francombe, "Polymorphism in lead metaniobate," *Acta Crystallographica*, vol. 9, pp. 683–684, 1956.
- [12] R. S. Roth, "Unit-cell data of the lead niobate, PbNb_2O_6 ," *Acta Crystallographica*, vol. 10, pp. 437–437, 1957.
- [13] C. V. Do Carmo, R. N. De Paula, J. M. Póvoa, D. Garcia, and J. A. Eiras, "Phase evolution and densification behavior of PBN ceramics," *Journal of the European Ceramic Society*, vol. 19, no. 6–7, pp. 1057–1060, 1999.
- [14] G. Burns, F. H. Dacol, R. Guo, and A. S. Bhalla, "Ferroelectric $(\text{Pb,Ba})\text{Nb}_2\text{O}_6$ near the morphotropic phase boundary," *Applied Physics Letters*, vol. 57, no. 6, pp. 543–544, 1990.
- [15] K. Sambasiva Rao, P. Murali Krishna, D. Madhava Prasad, and J. H. Lee, "Electrical and electromechanical properties of lead-potassium-yttrium-niobate ceramics-piezoelectric applications," *Journal of Physics and Chemistry of Solids*, vol. 70, no. 9, pp. 1231–1241, 2009.
- [16] K. R. Sahu and U. De, "Thermal characterization of piezoelectric and non-piezoelectric Lead Meta-Niobate," *Thermochimica Acta*, vol. 490, no. 1–2, pp. 75–77, 2009.
- [17] E. C. Subbarao, "X-ray study of phase transitions in ferroelectric PbNb_2O_6 and related materials," *Journal of the American Ceramic Society*, vol. 43, pp. 439–442, 1960.
- [18] V. L. Arantes, R. N. De Paula, I. A. Santos, D. Garcia, and J. A. Eiras, "Microstructure and densification behavior of $(\text{Pb,Ba})\text{Nb}_2\text{O}_6$ ceramics obtained by hot-pressing technique," *Journal of Materials Science Letters*, vol. 19, no. 18, pp. 1677–1679, 2000.
- [19] C. A. Randall, R. Guo, A. S. Bhalla, and L. E. Cross, "Microstructure-property relations in tungsten bronze lead barium niobate, $\text{Pb}_{1-x}\text{Ba}_x\text{Nb}_2\text{O}_6$," *Journal of Materials Research*, vol. 6, no. 8, pp. 1720–1728, 1991.
- [20] K. Okazaki and K. Nagata, "Effects of grain size and porosity on electrical and optical properties of PLZT ceramics," *Journal of the American Ceramic Society*, vol. 56, no. 2, pp. 82–86, 1973.
- [21] M. Roy, P. Dave, S. K. Barbar, S. Jangid, D. M. Phase, and A. M. Awasthi, "X-ray, SEM, and DSC studies of ferroelectric $\text{Pb}_{1-x}\text{Ba}_x\text{TiO}_3$ ceramics," *Journal of Thermal Analysis and Calorimetry*, vol. 101, no. 3, pp. 833–837, 2010.
- [22] P. Dave, M. Roy, S. K. Barbar, and S. Jangid, "Modulated DSC studies of $\text{Pb}_{1-x}\text{Ca}_x\text{TiO}_3$ ferroelectric ceramics," *Journal of Thermal Analysis and Calorimetry*, vol. 100, no. 3, pp. 937–940, 2010.
- [23] M. Roy, R. N. P. Choudhary, and H. N. Acharaya, "Differential scanning calorimetric studies of ferroelectric rare-earth molybdates," *Thermochimica Acta*, vol. 145, pp. 11–17, 1989.



Hindawi

Submit your manuscripts at
<http://www.hindawi.com>

